small-animal laboratory, adding a valuable asset to the pre-clinical research tool chest. As shown in the present study, micro-CT can provide accurate and precise measurements of the murine heart, and can serve as a useful adjunct to established measurements of cardiac function. Further refinements of this emerging technology are ongoing, and we predict that micro-CT scanning will continue to be used in the small-animal laboratory with increasing frequency.

Ahmad Y. Sheikh, MD, Koen E. A. van der Bogt, MD, Timothy C. Doyle, PhD, Maryam K. Sheikh, MD, Katherine J. Ransohoff, Ziad A. Ali, MD, Owen P. Palmer, MD, Robert C. Robbins, MD, Michael P. Fischbein, MD, PhD, *Joseph C. Wu, MD, PhD

*Department of Medicine, Division of Cardiology, Grant Building R140, Stanford, California 94305-5111. *E-mail: joewu@stanford.edu*

doi:10.1016/j.jcmg.2010.01.012

This study was funded by National Institutes of Health grants F32-HL-084982 (Dr. Sheikh), HL099117 (Dr. Wu), HL089027 (Dr. Wu), HL095571 (Dr. Wu), and HL093172 (Dr. Wu). Drs. Sheikh and van der Bogt contributed equally to this study.

REFERENCES

1. Nahrendorf M, Badea C, Hedlund LW, et al. High-resolution imaging of murine myocardial infarction with delayed-enhancement cine micro-CT. Am J Physiol Heart Circ Physiol 2007;292:H3172–8.
2. Detombe SA, Ford NL, Xiang F, Lu X, Feng Q, Drangova M. Longitudinal follow-up of cardiac structure and functional changes in an infarct mouse model using retrospectively gated micro-computed tomography. Invest Radiol 2008;43:520–9.
3. Pouleur AC, le Polain de Waroux JB, Kefer J, Pasquet A, Vanoverschelde JL, Gerber BL. Direct comparison of whole-heart navigator-gated magnetic resonance coronary angiography and 40- and 64-slice multidetector row computed tomography to detect the coronary artery stenosis in patients scheduled for conventional coronary angiography. Circ Cardiovasc Imaging 2008;1:114–21.
4. Ruzsics B, Lee H, Powers ER, Flohr TG, Costello P, Schoepf UJ. Images in cardiovascular medicine. Myocardial ischemia diagnosed by dual-energy computed tomography: correlation with single-photon emission computed tomography. Circulation 2008;117:1244–5.

▶APPENDIX

For supplementary figures and their legends, please see the online version of this article.

Angioscopy and OCT in Repeated In-Stent Restenosis in Saphenous Vein Graft

The morphological characteristics of in-stent restenosis (ISR) that occur in multiple layers of stents (stent in stent) are not well described. We used multimodality imaging in a 69-year-old man in whom repeated episodes of restenosis developed in a 9-year-old saphenous vein graft (SVG) to the left circumflex artery. He was initially treated with a sirolimus-eluting stent (SES) after the first

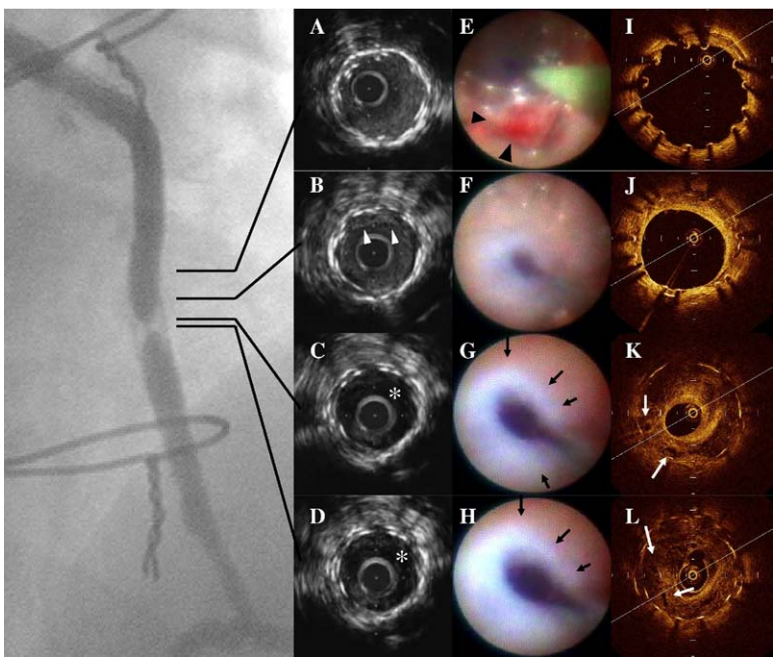

Figure 1. Comparison of IVUS, Coronary Angioscopy, and OCT Images of the Culprit Lesion

Although intravenous ultrasonography (IVUS) images of proximal sides were uncovered **(A)** or covered **(B)** by neointimal hyperplasia **(arrowheads)**, culprit lesions demonstrated an echolucent area **(*) (C, D)**. Angioscopic findings show uncovered stent struts with red thrombus **(black arrowheads)**, partially covered by neointima on the proximal side of the sirolimus-eluting stents **(E)**. Optical coherence tomography (OCT) image shows malapposed stent strut of sirolimus-eluting stents with or without neointima of stent strut and partially well apposed with neointima **(I)**. Angioscopy shows flesh-colored neointima-like coverage proximal to the culprit lesion **(F)**, and well apposed with high-intensity neointima by OCT **(J)**. Angioscopic findings of culprit lesions show sharply demarcated **(black arrows)** white coverage tissue **(G, H)**. OCT images of the same portions show a high-intensity layer. However, deep tissue is low intensity and contains some microchannels **(white arrows) (K, L)**. See Online Videos 1, 2, 3, and 4.

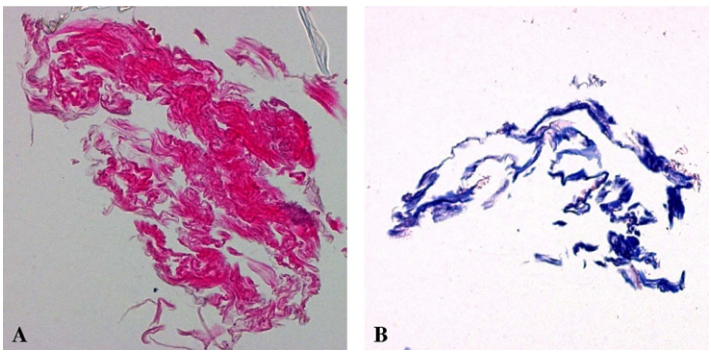

Figure 2. Pathological Findings Collected From the Culprit Lesion Showed Fibrin Clots

(A) Hematoxylin and eosin stain. **(B)** Phosphotungstic acid hematoxylin stain.

stenosis. Two years later, ISR developed that was treated with another SES. Once again, re-ISR developed 19 months later inside the SES that was implanted for ISR of the initial SES. Multimodality imaging (intravascular ultrasound [IVUS], coronary angioscopy, and optical coherence tomography [OCT]) were used (Fig. 1). IVUS showed the culprit lesion, which was an ISR lesion, to be echolucent tissue. Coronary angioscopy showed it to be sharply demarcated white tissue. OCT findings of the lesion showed that although the surface of the culprit lesion (which appeared as a white surface by angioscopy) was a signal-rich structure, underneath it contained a low signal and some microchannels in the deeper layer tissue. Percutaneous coronary intervention was performed with a distal protection device, and the pathological examination of the aspirate demonstrated fibrin clots (Fig. 2). Kume et al. (1) reported earlier that signal-rich structures without backscattering visualized by OCT are fibrin clots. The low-signal images in the deep tissue layer contained microchannels suggestive of organized thrombi. These results indicate that the white neointima-like coverage visualized by angioscopy after SES implantation could be a fibrin clot covering chronically formed thrombi, and that multimodality imaging could help in understanding the pathogenesis of ISR patterns after drug-eluting stent implantation.

***Tetsuya Fusazaki, MD, Tomonori Itoh, MD, Tatsuhiko Koeda, MD, Takumi Kimura, MD, Yoshinobu Ogino, MD, Hiroki Matsui, MD, Shoma Sugawara, MD, Motoyuki Nakamura, MD**

*Division of Cardiology, Department of Internal Medicine and Memorial Heart Center, Iwate Medical University School of Medicine, 1-2-1, Chuo-dori, Morioka City, 020-8505, Iwate, Japan. *E-mail: t_fusazaki@imu.ncvc.go.jp*

doi:10.1016/j.jcmg.2009.10.014

REFERENCE

1. Kume T, Okura H, Kawamoto T, et al. Fibrin clot visualized by optical coherence tomography. Circulation 2008;118:426–42.

APPENDIX

For supplementary videos and their legends, please see the online version of this article.

Fat Around the Heart

We are intrigued by the report of Cheng et al. (1) on pericardial fat volume as a predictor of increased death and disability for cardiovascular disease. Although the investigators were not able to distinguish epicardial fat from pericardial fat and consequently omitted a discussion on the prognostic value of epicardial fat in predicting premature death and disability from cardiovascular disease, the data are of great interest. Threshold values of epicardial fat thickness (measured by echocardiography) were established previously, and increased epicardial fat mass was proposed as a predictor of cardiovascular disease by Iacobellis et al. (2). Furthermore, current knowledge of epicardial and pericardial fat suggests that these 2 tissues have different metabolic and physiologic properties (3–5). Given the difference in the metabolic function and anatomical locations of epicardial and pericardial fat, it may be reasonable to ask the following 2 questions. First, does pericardial fat increase the atherosclerotic burden because of the known immunomodulatory function of white adipose tissue (6,7)? Secondly, does epicardial fat increase the chances of heart failure because of its anatomical proximity to the myocardium? We have reasoned previously that epicardial fat delivers substrate directly to the heart and sets the stage for myocardial steatosis, akin to visceral fat setting the stage for hepatic steatosis (8). In short, there remain many unanswered questions regarding the fat around the heart, but with the help of modern technologies, the answers may be just around the corner.

Sarah Yoder Thomas, MD, Romain Harmancey, PhD, *Heinrich Taegtmeyer, MD, DPhil

*Department of Internal Medicine, Division of Cardiology, University of Texas Houston Medical School, 6431 Fannin, Room MSB 1.246, Houston, Texas 77030. *E-mail: heinrich.taegtmeyer@uth.tmc.edu*

doi:10.1016/j.jcmg.2010.05.001

REFERENCES

1. Cheng VY, Dey D, Tamarappoo B, et al. Pericardial fat burden on ECG-gated noncontrast CT in asymptomatic patients who subsequently